Investigation of Autophagy-assisted Cell Death in Response to the Cancer Cell Toxin Coibamide A

by
Michelle Tan

A THESIS

submitted to

Oregon State University

University Honors College

in partial fulfillment of
the requirements for the
degree of

Honors Baccalaureate of Science in Biochemistry and Biophysics
(Honors Scholar)

Presented August 20, 2015
Commencement June 2016

AN ABSTRACT OF THE THESIS OF

Michelle Tan for the degree of Honors Baccalaureate of Science in Biochemistry and Biophysics presented on August 20, 2015. Title: Investigation of autophagy-assisted cell death in response to the cancer cell toxin coibamide A.

Abstract approved:

_____

Jane Ishmael

Autophagy, a homeostatic degradation pathway, has a role in promoting cell survival under stress conditions, but can also promote cell death under conditions of sustained stress. This project investigates the cytotoxic potential of coibamide A and other natural products in autophagy-deficient and wild-type mouse embryonic fibroblasts (MEFs). Wild-type MEFs were more vulnerable to coibamide A than cells lacking autophagy-related protein 5 (Atg5). Through cell viability assays and immunoblotting for markers of autophagy, it was found that restoration of expression of Atg5, a vital autophagy-related protein, in an autophagy-null background was able to partially restore the response characterized in wild-type MEFs. These results lend support to the existence of crosstalk between autophagy and apoptosis, and suggest coibamide A as a compound with characteristics that may utilize autophagy for pro-death signaling.

Key Words: Autophagy, natural products, cell death, coibamide A

Corresponding e-mail address: tanm@onid.oregonstate.edu

Investigation of Autophagy-assisted Cell Death in Response to the Cancer Cell Toxin Coibamide A

by
Michelle Tan

A THESIS

submitted to

Oregon State University

University Honors College

in partial fulfillment of
the requirements for the
degree of

Honors Baccalaureate of Science in Biochemistry and Biophysics
(Honors Scholar)

Presented August 20, 2015
Commencement June 2016

Honors Baccalaureate of Science in Biochemistry and Biophysics project of Michelle Tan presented on August 20, 2015.

APPROVED:

Jane Ishmael, Mentor, representing Pharmaceutical Sciences

Theresa Filtz, Committee Member, representing Pharmaceutical Sciences

Chrissa Kioussi, Committee Member, representing Pharmaceutical Sciences

Toni Doolen, Dean, University Honors College

I understand that my project will become part of the permanent collection of Oregon State University, University Honors College. My signature below authorizes release of my project to any reader upon request.

Michelle Tan, Author

INTRODUCTION

Macroautophagy (hereafter referred to as autophagy) is a cellular pathway in which intracellular components are catabolized via lysosomal degradation. It is a constitutive mechanism for maintaining cellular homeostasis. However, it also plays a part in a variety of other roles. For example, degraded cellular proteins from this pathway can be used in antigen presentation to induce an immune response (Nimmerjahn et al., 2003), or engulf invading bacteria (Gutierrez et al., 2004). Recent interest has fallen onto the role of autophagy as a stress response; whether such stress stems from an imbalance in cellular metabolism, the unfolded protein response, or pharmacological modulation, autophagy can serve to generate energy and nutrients and to remove damaged or misfolded proteins and organelles.

During autophagy, a double membraned vesicle envelops cellular components, forming an autophagosome. Fusion of this autophagosome with a lysosome allows degradation of captured contents. Many autophagy related genes (Atg) and their protein products have been identified (initially in yeast, then in mammalian cells). Through a cascade of ubiquitin-like conjugations involving some of these Atg proteins, Atgs 5, 12, and 16 create a complex that conjugates a phosphatidylethanolamine to LC3-I (Atg8 in yeast), yielding LC3-II (figure 1). This lipid-conjugated LC3-II is then inserted into both of the two autophagosome membranes, where its presence seems to control elongation of the membranes (Xie et al., 2008), and it is freed upon completion of the autophagosome (Nair et al., 2012). As such, LC3-II has been considered a reliable marker for autophagy (Mizushima,

2004). Moreover, when ATG5 is knocked down or made defective, LC3-I conversion is no longer observed (Mizushima et al., 2001).

On another front, the inactivation of mammalian target of rapamycin (mTOR), a consequence of a low energy state within the cell (i.e., low ATP), activates the ULK1 complex which is known to play a role in initiating autophagy. This branch of the pathway is termed mTOR-dependent autophagy. Meanwhile, mTOR-independent autophagy is initiated via alternative methods. One of these is ER stress, which leads to the unfolded protein response (Sarkar, 2013). As misfolded proteins accumulate, the UPR triggers a variety of pathways, one of which is autophagy - presumably upregulated to assist in degradation (Matus et al., 2008).

All in all, the autophagic mechanism is one thought to confer enhanced durability to the stressed cell. In one illustrative study, apoptosis-resistant, non-proliferating cells were deprived of a vital growth factor, thus causing cell-surface nutrient transporters to be internalized and nutrient deficiency to ensue (Lum et al., 2005). While in this starvation state, cells were able to survive for upwards of six weeks, while maintaining extensive autophagic activity. However, when autophagy was inhibited (either genetically or pharmacologically), cell viability in these conditions dropped to mere days. Thus, the pathway in question is highly implicated in the tolerance of cells to metabolic stresses.

This would also hold true in the context of cancer cells, potentially to the detriment of our present cancer therapies. However, the link between cancer and autophagy is quite complex and our understanding of it is still incomplete. The relevance of this relationship may be increased by the nature of environment experienced by a cancer cell – the inner regions of a tumor are prone to hypoxia and nutrient deficiency due to insufficient circulation, leading to a deficit in ATP produced and generating stress on the cells in the area. Meanwhile, the cancerous cell itself will be more demanding of nutrients and energy in its uncontrollably proliferative state. It has been shown that cells that have suffered oncogenic Ras activation maintain a concomitant activation of the autophagy pathway in order to sustain the high anabolic rate of the transformed cell (Guo et al., 2011).

At the same time, the paradigm of autophagy as homeostatic/ stress survival mechanism also implies that defects in the pathway are met with the induction of disease states – among these are neurodegenerative diseases (e.g., Parkinson's, Alzheimer's), and infection (via disruption at the intersection of autophagy and the immune response), and cancer. Indeed, in this final case, metabolic stresses usually mitigated by autophagic processes instead promote tumorigenesis (Mathew et al., 2007).

Meanwhile, a connection between autophagy and cell death has also been observed. A form of programmed cell death designated as distinct from apoptosis, called "autophagic cell death," is associated with induction of autophagy that serves as a death mechanism. A definition of autophagic cell death (to set it apart from apoptosis

and other forms of non-apoptotic cell death) has evolved over the years as the characterization shifted from a morphological description to one based on molecular markers. Morphologically, a hallmark of autophagic cell death was considered to be the appearance of autophagosomes engulfing cytoplasm and organelles, although it has also been noted that chromatin condensation happens later than it would in apoptosis (Gozuacik & Kimchi, 2007). One marker-based set of criteria, proposed by Shen and Codogno, defines autophagy mediated cell death as cell death such that it occurs without caspase and apoptotic machinery activation, it creates an increase of flux through the autophagic pathway, and it can be prevented through pharmacological and genetic inhibition of autophagy (Shen & Codogno., 2011). Distinguishing between autophagy serving a pro-survival role or autophagic cell death has also been an area requiring further investigation – one perspective proposes that the difference lies in the regulation of autophagy related proteins (Tsujimoto & Shimizu, 2005).

Ultimately, the usefulness of autophagy as a target for cancer therapy has not been tapped, due to the complex dependence of the relationship on the individual cancer cell's metabolic demands and its tumor environment. In the greater scheme of disease progression, autophagy could play a role in either tumor growth or suppression, depending on the stage of cancer.

Coibamide A is a lead structure with anti-cancer potential discovered and isolated from a marine cyanobacterium by Dr. Kerry McPhail as part of the International

Cooperative Biodiversity Groups (ICBG) program based in Panama (Medina et al., 2008). In their producing organisms, natural products are secondary metabolites providing some survival advantage (for example, toxicity to predators, prey, or competition). For humans, these natural products have historically presented opportunities for drug development, to the point of constituting or inspiring the majority of approved drugs. Often, newly discovered natural products also possess novel mechanisms of action (Li & Vederas, 2009).

The primary mechanism of action of coibamide A is under investigation, although it is known to induce mTOR-independent autophagy in mouse embryonic fibroblasts (MEFs) and human cancer cells (Hau et al., 2013). Autophagy is upregulated within an hour of coibamide A exposure but is not required for cell death; MEFs lacking Atg5, an essential component of the autophagy pathway, eventually undergo apoptosis (Hau et al., 2013). Surprisingly, autophagy-deficient MEFs were routinely found to be slightly less vulnerable to coibamide A than wild-type cells, raising the possibility that the autophagy pathway serves to promote cell death in response to coibamide A. This project will focus on analysis of coibamide A-induced cell death in wild-type (WT) and matched, autophagy-deficient, Atg5 knockout (Atg5 KO) MEFs to test the hypothesis that Atg5 accelerates the rate of cell death in response to coibamide A.

MATERIALS AND METHODS

Reagents

Isolation of coibamide A was described previously (Medina et al., 2008), as was the isolation of apratoxin (Thornburg et al., 2013). Rapamycin, thapsigargin, and tunicamycin were obtained commercially from Sigma-Aldrich. General reagents not otherwise noted were obtained from Sigma-Aldrich and VWR.

Cell culture

Cells were incubated at 37°C, 5% CO_2. DMEM formulation listed in appendix. To subculture, media was aspirated, the surface was washed with PBS (Appendix), 0.25% Trypsin (Mediatech Inc., #25-053-CI) was used to detach cells (about 0.025mL per cm^2). The resulting suspension was quenched with media (3x trypsin volume), and diluted to an appropriate cell density into a new flask/plate such that 90% confluency would be reached in 48h. At the minimum, if confluency was not reached, media was refreshed every 48 h.

Cell lysates

To treat cells to be used for cell lysates, cells were plated in dishes, allowed to settle onto the plate, and then treated hours before collection (allowed to incubate in the presence of compound of interest). A 0.1% DMSO treatment was used as vehicle control.

Lysates were collected from plates (either 6cm or 10cm) on ice after treatment. Plates were aspirated of media and washed with PBS (Appendix), and lysis buffer

(Appendix) (60uL or 120uL) was applied. Cells were scraped off, collected, and centrifuged (20,000rpm for 20min). Supernatant was then collected, normalized, and used in SDS-PAGE.

Normalization of samples for protein content

A 1:10 dilution of each cell lysate was done (in duplicate) on a 96-well plate (2uL lysate, 18uL ddH2O), standardized against an 8 point ladder ranging 0 - 0.7mg/mL BSA. Five parts addition of BCA reagent (Thermo Sci. # 23228, #23224) mixed according to manufacturer's protocol, incubation for 30min, and absorbance reading at 562nm gave concentrations of samples.

Most samples were then diluted to 25μg/20uL in 3x Laemmli buffer (Appendix) and lysis buffer.

SDS-PAGE and western blotting

Gels were 12.5% polyacrylamide for the resolving layer with a 4.5% stacking gel (Appendix).

In running buffer (Appendix), gels were loaded with sample and run for 15min at 100V and an appropriate amount of time to resolve bands at 160V (~60min). In transfer buffer (Appendix), protein was transferred to a PVDF membrane (Thermo Scientific, #88518) at 95V for 90min.

Blocking step was in 5% dry milk (w/v) in TBST (Appendix) for 60min at room temperature. Three 5min wash steps followed, and blots were incubated in primary

antibody at 4°C overnight (~16h). Primary antibody was an appropriate dilution of stock antibody in 5% BSA in TBST.

After incubation, blots were given three 5min washes in TBST, 60min in appropriate secondary antibody (goat anti-rabbit, 1:7500 in 5% dry milk in TBST), and three more 5min washes in TBST.

Primary and secondary antibodies were obtained from Cell Signaling Technology, listed as follows, with item code and working dilution: GAPDH (8884, 1:30,000), LC3 A/B (4108, 1:1000), 4E-BP1 (9452, 1:2000), CHOP (5554, 1:1000), Atg5 (12994, 1:2000), Goat anti-Rabbit secondary (2125, 1:2000).

Chemiluminescent detection was done with ECL (GE Healthcare, RPN2236 and RPN2232) according to manufacturer's instructions, captured on film (VWR, 11299-020), and developed (developer: Carestream #1902485, fixer: Carestream #1900984).

Stripping and reprobing

When applicable, stripping and reprobing a blot consisted of 4x 5min TBST washes, a 30min wash in stripping buffer (appendix), and 6x 5min TBST washes. Primary antibody incubation followed as normal.

Endpoint cell viability assays/ Concentration-response curves

Endpoint assays were performed in 96-well plates. Cells were seeded at a density of 20000 cells/well with 50uL of media/well, allowed to incubate for 18h, and then treated (adding another 50uL/well). After a set amount of time, WST-8 (Cayman

Chemical, #10010199) was used according to manufacturer's specifications in order to quantitate remaining viable cells against vehicle.

Concentration-response curves were done over an appropriate range of concentrations for each compound of interest in order to characterize a sigmoid plot. Each condition was done in triplicate, excepting the vehicle (0.1% DMSO), which was done with 12 replicates. Dilutions were made up from stock (in DMSO) via serial dilution (also in DMSO) and then further diluted into serum-free media before addition to the wells. Data was analyzed using Graphpad Prism 5 software with nonlinear regression and fit to a logistic curve. Unpaired t-tests were used to determine statistical significance for the endpoint assay described in figure 5.

Trypan blue exclusion assay

Plates were seeded at 3000 cells per well, treated with coibamide A (3nM and 10nM) 18h afterwards, and time points were taken from 0 to 48 h after treatment. At each collection point, wells were aspirated, detached using trypsin (0.25%), quenched with serum-free media, and collected. Trypan blue reagent (Mediatech Inc., 25-900-Cl) was added at a volume equal to that of media added, and cell counts were obtained via hemocytometer. The number of cells still viable was compared to a DMSO (0.1%) treated well collected at the same time.

Cell line purification

A heterogeneous population of Atg5 KO and Atg5 KO transfected with Atg5-GFP (herein referred to as the "Atg5-GFP" cell line) was gifted by Dr. Ian Ganley,

University of Dundee, Scotland (Ganley et al., 2011). In order to isolate Atg5-GFP cells in the population, the population was plated onto a 20cm dish at heavy dilution, such that individual cells would form homogeneous colonies. Colonies were collected, and a further limiting dilution was done with each colony. All throughout, blasticidin (Life Technologies, R21001), (an antibiotic with a resistance gene in the transfected plasmid) was added to media at a concentration of 10mg/mL (in water) in order to maintain the presence of the plasmid.

Immunofluorescence, immunocytochemistry

As the transfected cells expressed GFP-conjugated Atg5, fluorescence microscopy was used to roughly determine the presence of Atg5-expressing cells within the cell line after purification.

Slides for immunocytochemistry were made by preparing glass slides in culture dishes. As the treatment was a 4h starvation, media in dishes was replaced with EBSS (Hyclone Laboratories, SH30029.02) (three washes were performed before finally allowing the cells to incubate for the treatment).

Slides were fixed (2x PBS washes, 1x 20 min 3.7% formaldehyde + 10mM HEPES in DMEM incubation at room temperature, 2x 10mM HEPES in DMEM washes, 1x 10 min HEPES-DMEM incubation at room temperature), and stained with LC3 antibody (same as used in immunoblotting, 1:500 dilution) (follow previous sequence with 2x PBS washes, 3 min 0.2% NP-40 in PBS incubation at room temperature, 2x 1% BSA in PBS (hereafter "BSA-PBS") washes, 1x 15 min BSA-PBS incubation with agitation at room temperature, 1x 1h BSA-PBS + antibody incubation at 37C, 3x

10min BSA-PBS washes with agitation, 1x 30 min BSA-PBS + secondary antibody incubation at room temperature in darkness, 3x 10 min BSA-PBS washes with agitation in dark). Mounting medium was prolong gold with DAPI (Invitrogen, P36935). Finally, slides were viewed at 66x magnification, overlaying GFP, DAPI, and the secondary antibody (Alexa fluor 594) (Abcam, #ab6939) channels to obtain pictures.

RESULTS

Previous analyses of coibamide A-induced cytotoxicity showed that an autophagy response is not needed to trigger apoptosis in MEFs (Hau et al., 2013); however, the rate of cell death may be accelerated in the presence of a functional autophagy pathway. To pursue this observation, we used a basic cell viability in which the ability of the WT and Atg5-null MEFs to exclude Trypan blue was monitored for up to 48 h after exposure to fixed concentrations of coibamide A (Figure 2A). In these studies, coibamide A induced a time-and concentration-dependent loss in membrane integrity relative to control cells, in that wild-type cells were more vulnerable than Atg5 KO MEFs. The higher sensitivity of the Atg5 WT MEFs to coibamide A exposure could also be seen morphologically by 24 and 36h, in agreement with Trypan blue exclusion assay data, with more cells rounding and beginning to float off the plate than were observed in the corresponding Atg5-null MEFs (figure 2B).

Two well characterized pharmacological inducers of ER stress, thapsigargin and tunicamycin also induce mTOR-independent autophagy. We therefore compared the action of these two natural products in ATG5 WT and KO MEFs to that of coibamide A. Wild-type MEFs were first treated with a fixed concentration of coibamide A (30nM), rapamycin (100μM), thapsigargin (10μM), tunicamycin (20μg/mL) or vehicle (0.1% DMSO) and whole cell lysates collected for immunoblot analysis. All four compounds induced accumulation of LC3-II, yet only rapamycin caused a shift in the molecular weight of 4E-BP1, confirming that coibamide A, thapsigargin and tunicamycin all induce autophagy without engaging mTOR signaling (Figure 3).

Meanwhile, thapsigargin and tunicamycin induced expression of CAAT-enhancer-binding protein homologous protein (CHOP) (Figure 3). CHOP is here used as a selective marker for ER-stress, as its expression is one outcome of the unfolded protein response (UPR) – its expression helps lead the cell to apoptosis (Marciniak, 2004). In contrast, we observed no CHOP expression in WT MEFs following exposure to coibamide A, suggesting that coibamide A does not act as a classic inducer of ER stress and thus mTOR-independent autophagy is initiated by a different mechanism.

Cytotoxicity in coibamide A-treated MEFs was next compared to the viability of MEFs treated for 48 h with rapamycin, thapsigargin, tunicamycin or vehicle (0.1% DMSO) (Figure 4). Concentration response analyses of ATG5 WT and KO MEFs consistently showed a differential sensitivity of the two cell lines to coibamide A, with WT MEFs being the more sensitive (Figure 4A; Table 2). This trend was not observed with the other three compounds (Figure 4B-D). Rapamycin was not cytotoxic to either cell line, while KO MEFs were more sensitive to both pharmacological inducers of ER stress (Figure 4B-D; Table 2).

We next compared the action of coibamide A to that of apratoxin A. Apratoxin A is another natural product isolated from a marine cyanobacterium but is generally more cytotoxic to cells than coibamide A (unpublished results). For these studies, MEFs were treated for 24 h with, coibamide A (30nM), apratoxin A (30nM), thapsigargin (10μM), or vehicle (0.1% DMSO) and cell viability assessed using the same endpoint

assay. Apratoxin A seemed to behave much like coibamide A in these studies (Luesch et al., 2001). Both natural products were observed to induce autophagy, while not causing an increase in CHOP expression (figure 5B), and also eliciting greater cell death in WT MEFs than in KO MEFs (figure 5C).

To investigate the role of autophagy in coibamide A or apratoxin A-induced cell death, a line of Atg5 KO MEFs transduced to express Atg5-GFP was generated. Western blots showed the expression of Atg5 in this cell line, albeit at a higher molecular weight, due to the added GFP tag (27kDa) (figure 6A). Accordingly, these Atg5-GFP expressing MEFs also showed a restored LC3 lipidation pathway, as shown by the presence of LC3-II in response to induction of autophagy following rapamycin treatment (figure 6A). Preliminary immunostaining of Atg5-GFP MEFs with an anti-LC3 antibody suggested the presence of GFP-tagged Atg5, as well as a punctate LC3-II distribution, a marker for autophagy (figure 6B). Though higher resolution images will be needed to fully validate this response, our preliminary findings indicate that Atg5 KO MEFs undergo appropriate autophagy signaling when Atg5-GFP is re-expressed.

We then treated Atg5-GFP MEFs with increasing concentrations of either coibamide A or apratoxin A alongside WT and KO MEFs for 24h. Preliminary concentration-response analyses suggest that the Atg5-GFP MEF cell line possesses an intermediate sensitivity to coibamide A relative to WT and KO cells, or a partial recapitulation of the Atg5 WT phenotype (Figure 7). As re-expression of Atg5 in KO cells did not

fully restore the wild-type phenotype, further studies will be needed to determine if an intact autophagy pathway contributes to accelerated cell death in response to coibamide A.

DISCUSSION

Coibamide A was previously found to elicit concentration-dependent cell death in both Atg5 WT and Atg5 KO MEF cell lines, but with a more potent effect in WT MEFs. For this study, MEF cells were selected for experiments, as these are convenient cells for studying autophagy; cell lines lacking essential components of the autophagy pathway have already been generated. In the present study, we captured morphological features, performed cell viability assays and analyzed expression of autophagy and ER stress biomarkers to investigate a potential role for autophagy as a mediator of cell death in response to coibamide A.

The connection between autophagy and cell death has been previously noted in crosstalk between autophagy and apoptosis, wherein the former initiates signaling for the latter. Of particular interest to this project, cleavage of Atg5 by calpain has been found to produce a fragment that migrates to the mitochondria, releases cytochrome c, and initiates caspase-mediated apoptosis (Yousefi et al., 2006). It has also been suggested that autophagy provides support for apoptosis progression, supplying energy for the remodeling required – membrane blebbing, chromatin condensation, etc. (Eisenberg-Lerner et al., 2009).

This crosstalk potentially gives a broader context to the differential sensitivity reported here – if the lower sensitivity to coibamide A observed in Atg5 KO MEFs is a result of missing a piece in the apoptotic pathway, Atg5-GFP MEFs would

theoretically restore that apoptosis, thereby restoring the enhanced cell death observed in WT MEFs.

In comparing various natural products within the scope of this study, similarities between the coibamide A response and the apratoxin A response were consistent through the extent of testing. Both were observed to induce mTOR-independent autophagy that is not explained by ER stress, and also be more cytotoxic to WT MEFs over KO MEFs, suggesting a similar mechanism of action. Given these commonalities, an autophagy-dependent rate of cell death favoring the autophagy-deficient may be a theme among a yet undefined subset of natural products.

On assaying cell viability with both coibamide A and apratoxin A treatment, a response intermediate to the WT and KO cells was observed in the Atg5-GFP MEFs. Whether this represents an artefact of a heterogeneous cell line in which transfection and purification efficiency was less than complete or if there is another factor at work remains to be seen.

A limitation of our study is that MEFs are generally very vulnerable to coibamide A and apratoxin A and thus relatively small differences in the rate of cell death were difficult to measure. Future work would investigate relative levels of N-terminal Atg5 present, as well as manipulation of the apoptotic pathways in order to probe the autophagy-apoptosis crosstalk involved in cell death and determine its contribution to the effect described previously.

While the application of autophagy modulation to cancer therapy remains complex, these two compounds, coibamide A and apratoxin A, may present a novel means of manipulating a pathway and its ultimate consequence, cell death. Although the cytotoxicity of both is such that they might never reach the status of being used as therapeutic agents, they may provide an entry point into investigating autophagy-apoptosis crosstalk further as molecular probes.

Figure 1. Relevant cell signaling pathways leading to autophagy, both mTOR-dependent and mTOR-independent

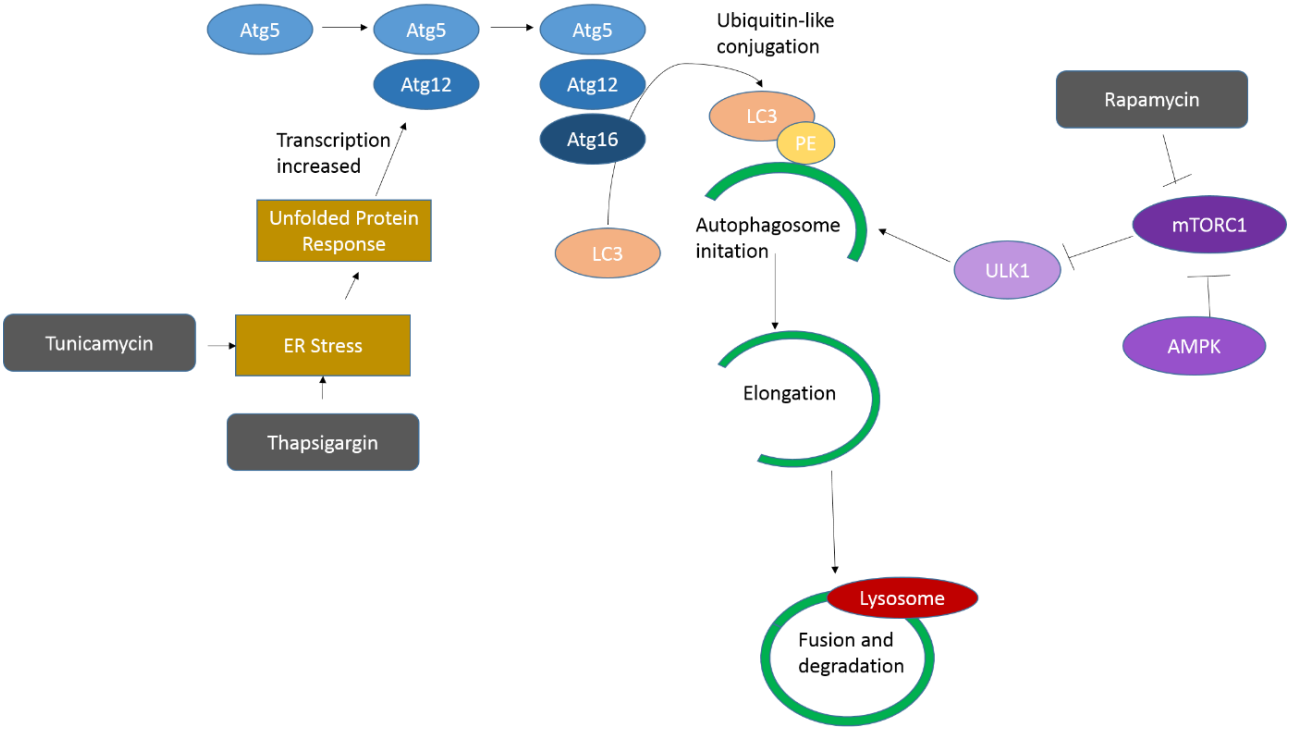

Figure 2. Wild-type MEFs are more vulnerable than Atg5-null MEFs to coibamide A-induced cytotoxicity.

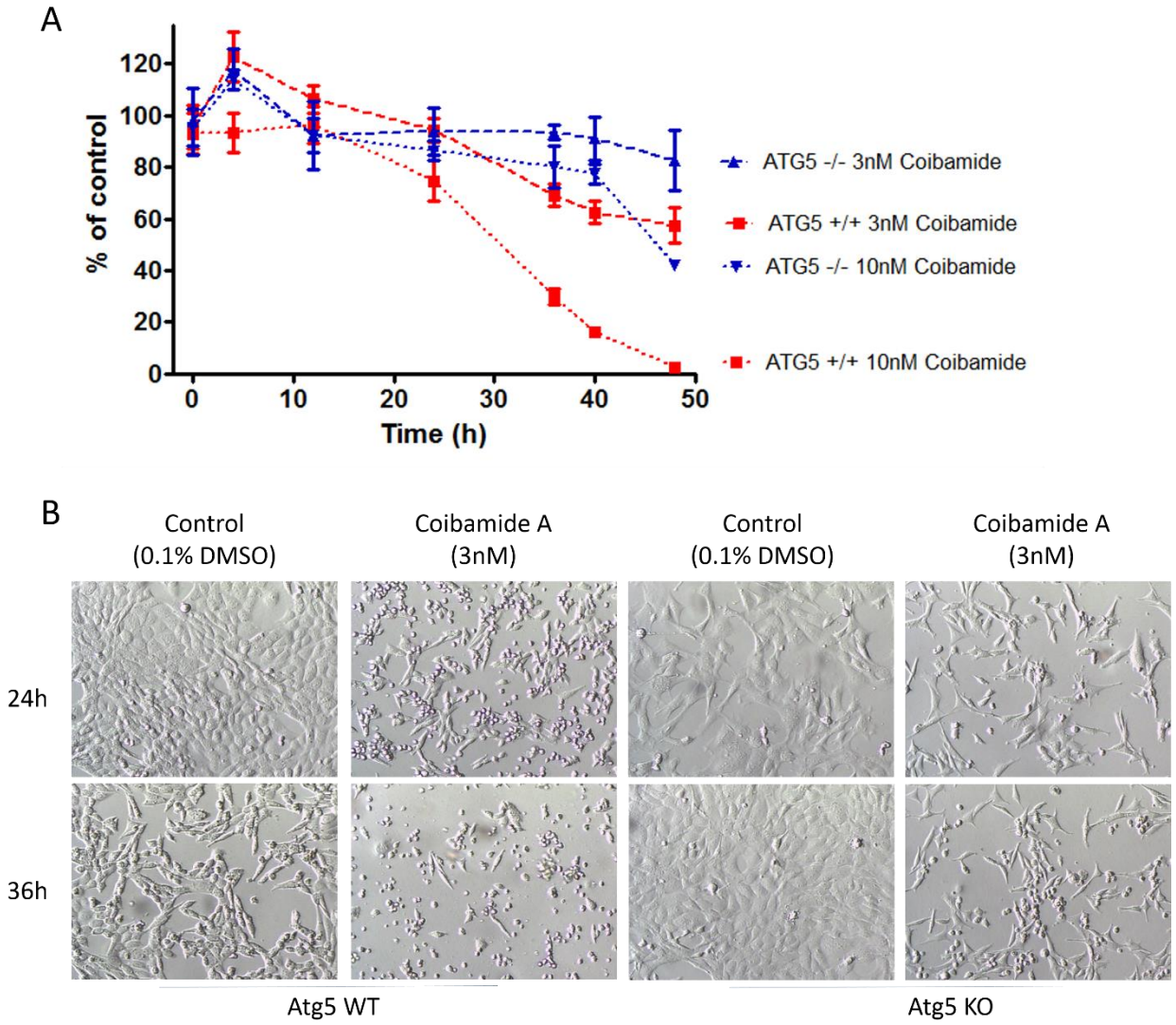

A) Trypan Blue exclusion assay data - Atg5 WT and KO cell lines were treated at two coibamide A concentrations (3nM and 10nM) for 0-48h, and viable cell count was compared to 0.1% DMSO control

B) Time course of Atg5 WT and KO MEFs at 24, and 36 hours treated with 0.1% DMSO (left) or 3nM coibamide A (right)

Figure 3. Coibamide A is not a classic inducer of ER-stress.

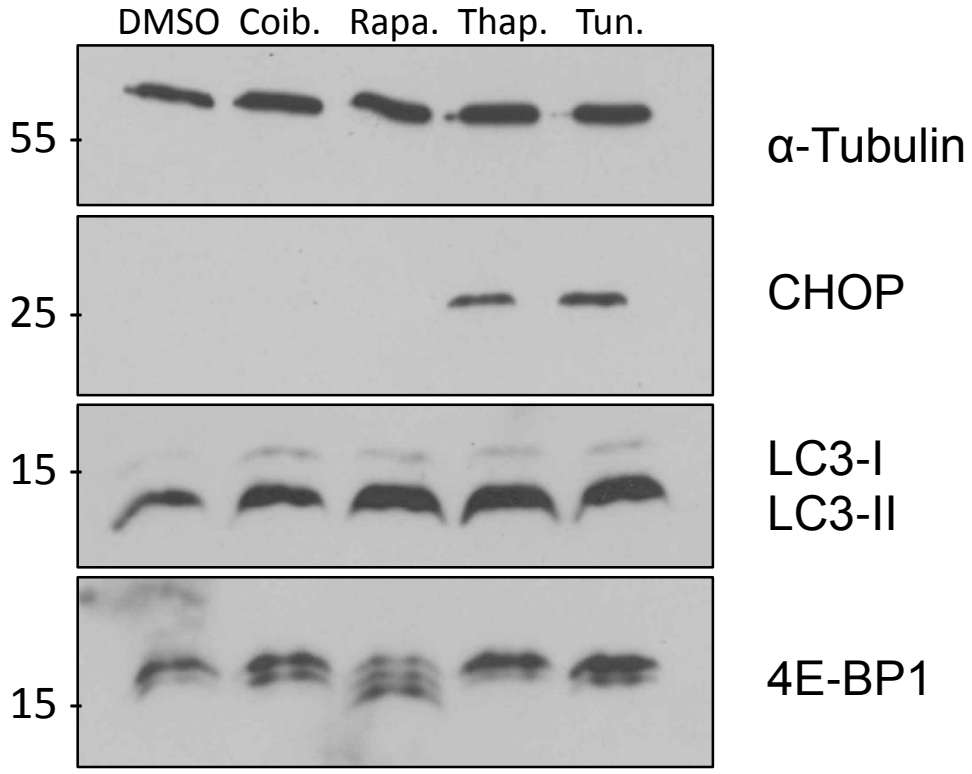

Immunoblot for alpha-Tubulin (loading control), CHOP, LC3-I/LC3-II, and 4E-BP1 in ATG5 WT MEFs with 4h treatments of DMSO (0.1%), coibamide A (30nM), rapamycin (100μM), thapsigargin (10μM), and tunicamycin (20μg/mL). (representative of 3 independently run blots)

Figure 4: Comparison of cell viability in wild-type and Atg5-null MEFs in response to coibamide A, rapamycin and pharmacological inducers of ER stress

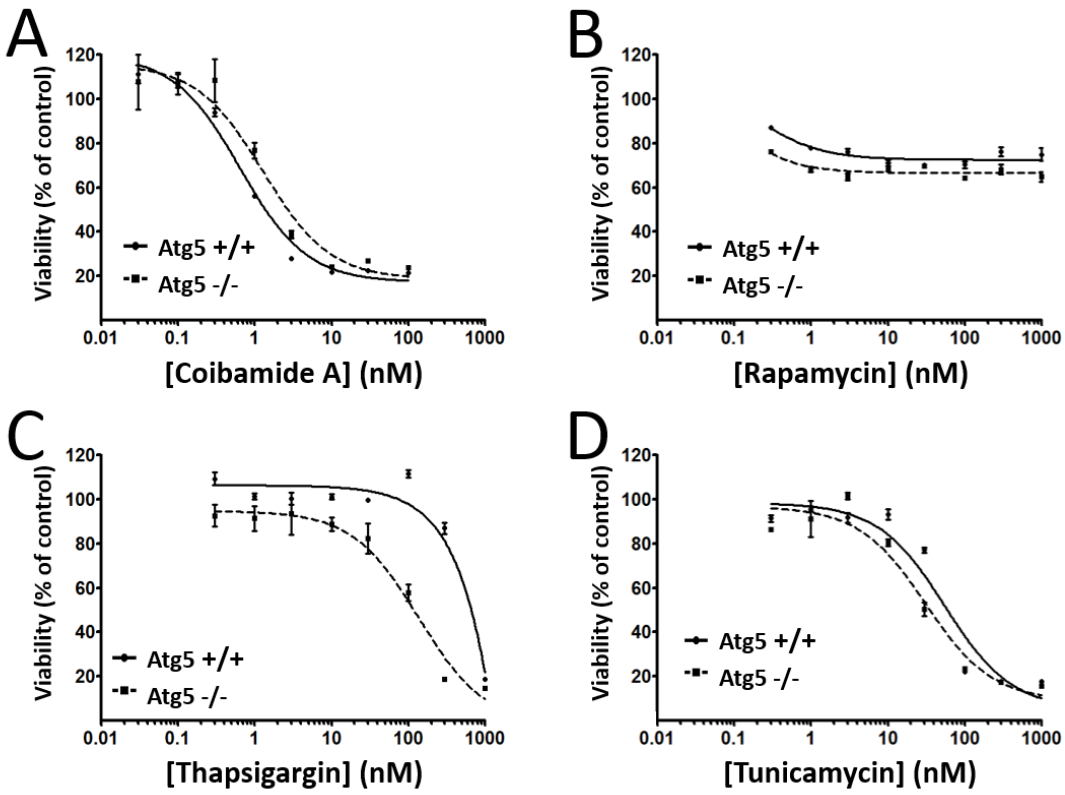

48h endpoint assays with coibamide A and other natural products in Atg5 WT (solid line) and Atg5 KO (dashed line) cells, representative of 4 independent experiments. EC_{50} values are listed in table 2

Figure 5. The cyanobacterial metabolite apratoxin A elicits a similar pattern of responses to coibamide A

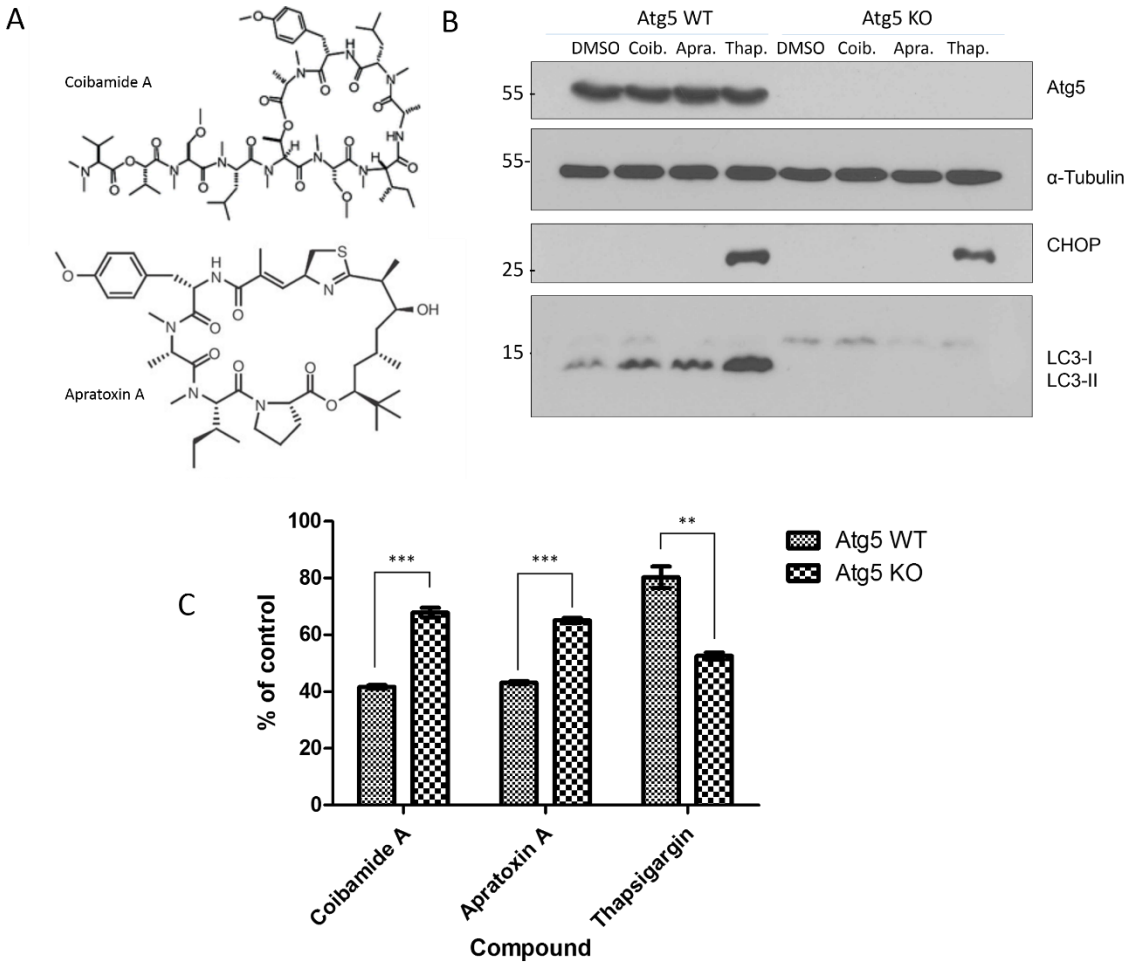

A) Structure of coibamide A (top) and apratoxin A (bottom)

B) Immunoblot for Atg5, alpha-Tubulin (loading control), CHOP, and LC3-I/LC3-II in ATG5 WT and KO MEFs with 4h treatments of DMSO (0.1%), coibamide A (30nM), apratoxin A (30nM), and thapsigargin (10μM) (representative of 3 independently run blots)

C) Histogram comparing endpoints in Atg5 WT and KO MEFs at the highest treatment concentration after 24h in coibamide A (100nM) ($p = 0.0001$), apratoxin A (100nM) ($p < 0.0001$), and thapsigargin (1μM) ($p = 0.0023$).

Figure 6. Characterization of Atg5 null MEFs stably expressing Atg5-GFP.

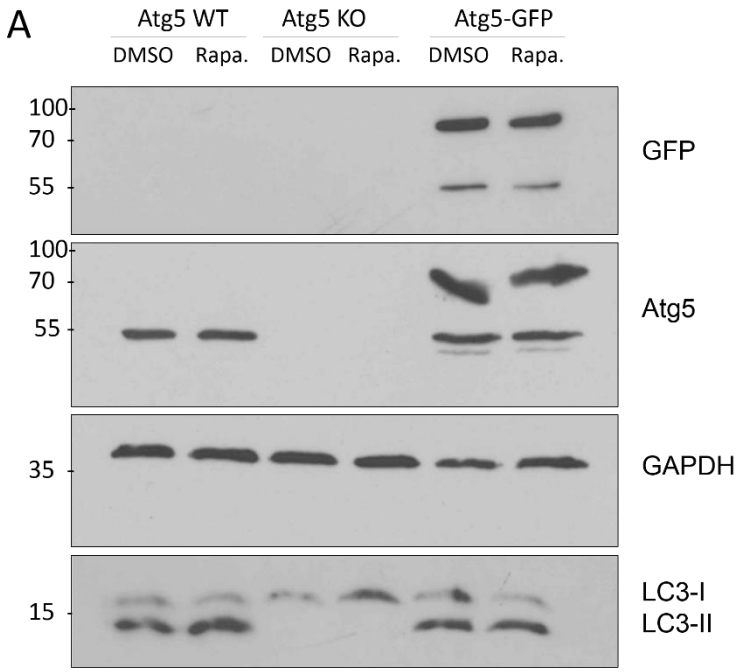

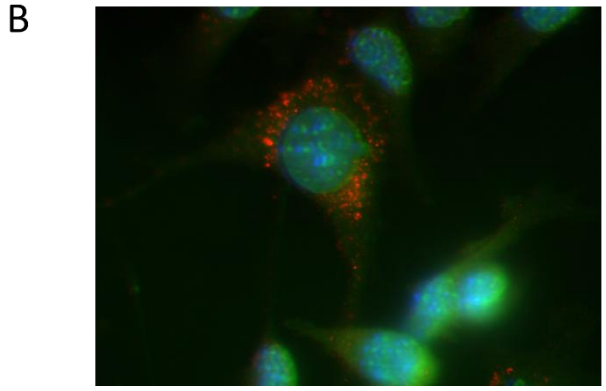

A) Immunoblot forAtg5, GAPDH (loading control), and LC3-I/LC3-II in Atg5 WT, KO, and GFP MEFs with 4h treatments of DMSO (0.1%) and rapamycin (100μM). (representative of 3 independently run blots)

B) Overlay picture of GFP, DAPI, and LC3 antibody stained channels of 4h starved Atg5-GFP MEFs fixed on slide at 66x magnification.

Figure 7. Re-expression of Atg5-GFP partially rescues the wild-type phenotype in response to coibamide A

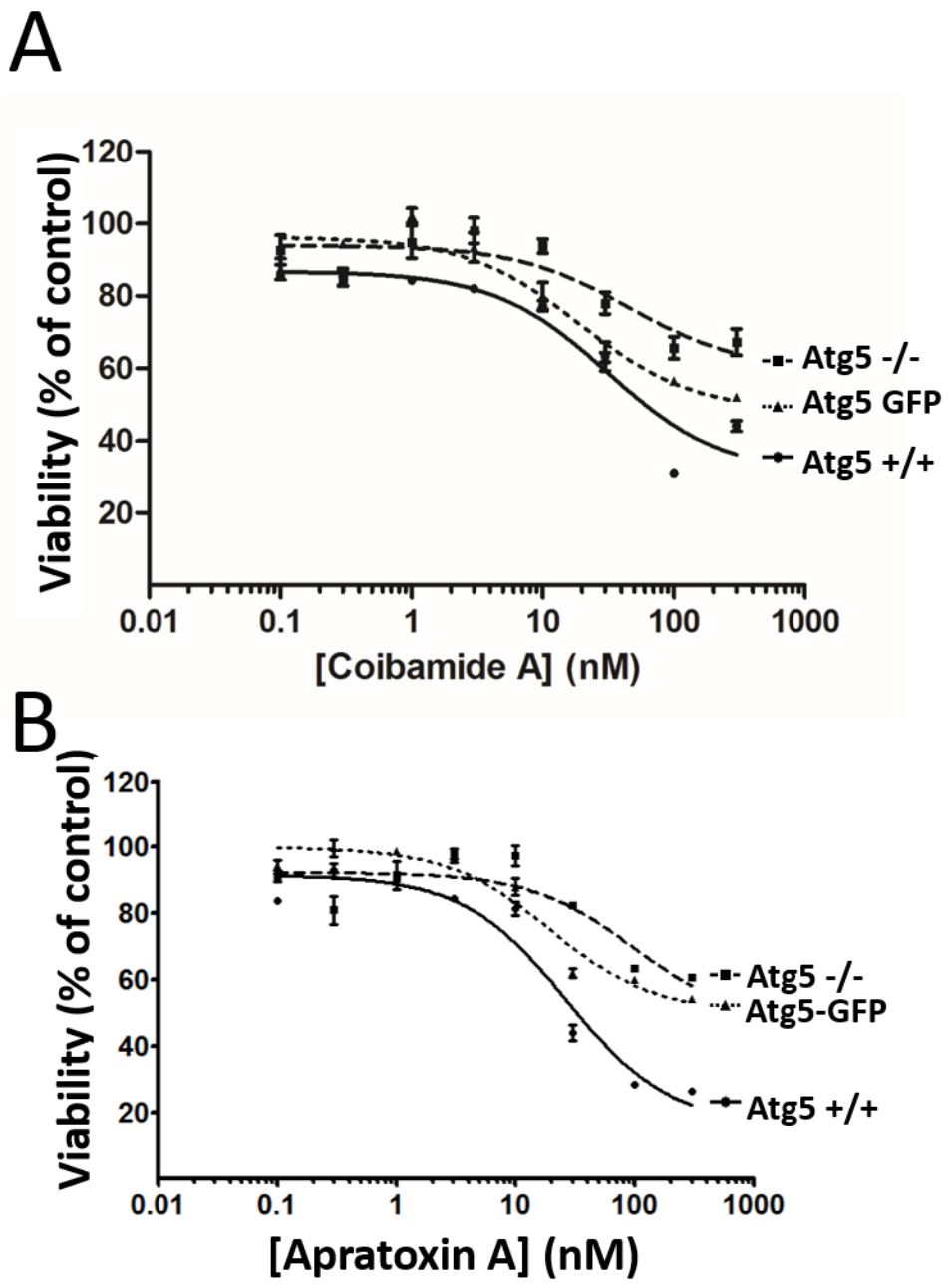

Concentration-response curves in Atg5 WT, KO and GFP MEFs with A) coibamide A and B) apratoxin A

Compound	Autophagy mTOR dependency	Mechanism of Action
Coibamide A	Independent	Putative Secretory Pathway inhibitor
Apratoxin A	Independent	Secretory pathway inhibition[18]
Thapsigargin	Independent	ER Stress[19]
Tunicamycin	Independent	ER Stress[20]
Rapamycin	Dependent	mTOR inhibitor[21]

Table 1: Modulators of autophagy and their mechanisms to be used in comparison to coibamide A

Compound	**Atg5 WT**		**Atg5 KO**	
	EC_{50}	**95% CI**	**EC_{50}**	**95% CI**
Coibamide A	**1.1254**	**0.4838 – 2.698**	**1.61725**	**0.7070 – 2.950**
Rapamycin	**Not determined**	**Not determined**	**Not determined**	**Not determined**
Thapsigargin	**61.93**	**13.5 – 237.0**	**59.782**	**16.75 – 255.2**
Tunicamycin	**52.27**	**27.51 – 96.00**	**40.2**	**18.64 – 89.82**

Table 2: Comparison of EC_{50} values in Atg5 WT and Atg5 KO MEFs.

REFERENCES

Eisenberg-Lerner, A., Bialik, S., Simon, H. U., & Kimchi, A. (2009). Life and death partners: apoptosis, autophagy and the cross-talk between them. *Cell Death & Differentiation*, *16*(7), 966-975.

Ganley, I. G., Wong, P. M., Gammoh, N., & Jiang, X. (2011). Distinct autophagosomal-lysosomal fusion mechanism revealed by thapsigargin-induced autophagy arrest. *Molecular cell*, *42*(6), 731-743.

Gozuacik, D., & Kimchi, A. (2007). Autophagy and cell death. *Current topics in developmental biology*, *78*, 217-245.

Gutierrez, M. G., Master, S. S., Singh, S. B., Taylor, G. A., Colombo, M. I., & Deretic, V. (2004). Autophagy is a defense mechanism inhibiting BCG and Mycobacterium tuberculosis survival in infected macrophages. *Cell*, *119*(6), 753-766.

Guo, J. Y., Chen, H. Y., Mathew, R., Fan, J., Strohecker, A. M., Karsli-Uzunbas, G., ... & White, E. (2011). Activated Ras requires autophagy to maintain oxidative metabolism and tumorigenesis. *Genes & development*, *25*(5), 460-470.

Hau, A. M., Greenwood, J. A., Löhr, C. V., Serrill, J. D., Proteau, P. J., Ganley, I. G., ... & Ishmael, J. E. (2013). Coibamide A induces mTOR-independent autophagy and cell death in human glioblastoma cells.

Heifetz, A., Keenan, R. W., & Elbein, A. D. (1979). Mechanism of action of tunicamycin on the UDP-GlcNAc: dolichyl-phosphate GlcNAc-1-phosphate transferase. *Biochemistry*, *18*(11), 2186-2192.

Li, J. W. H., & Vederas, J. C. (2009). Drug discovery and natural products: end of an era or an endless frontier?. *Science*, *325*(5937), 161-165.

Liu, Y., Law, B. K., & Luesch, H. (2009). Apratoxin A reversibly inhibits the secretory pathway by preventing cotranslational translocation. *Molecular pharmacology*, *76*(1), 91-104.

Luesch, H., Yoshida, W. Y., Moore, R. E., Paul, V. J., & Corbett, T. H. (2001). Total Structure Determination of Apratoxin A, a Potent Novel Cytotoxin from the Marine Cyanobacterium Lyngbya m ajuscula. *Journal of the American Chemical Society*, *123*(23), 5418-5423.

Lum, J. J., Bauer, D. E., Kong, M., Harris, M. H., Li, C., Lindsten, T., & Thompson, C. B. (2005). Growth factor regulation of autophagy and cell survival in the absence of apoptosis. *Cell*, *120*(2), 237-248.

Matus, S., Lisbona, F., Torres, M., León, C., Thielen, P., & Hetz, C. (2008). The stress rheostat: an interplay between the unfolded protein response (UPR) and autophagy in neurodegeneration. *Current molecular medicine*, *8*(3), 157-172.

Marciniak, S. J., Yun, C. Y., Oyadomari, S., Novoa, I., Zhang, Y., Jungreis, R., ... & Ron, D. (2004). CHOP induces death by promoting protein synthesis and oxidation in the stressed endoplasmic reticulum. *Genes & development*, *18*(24), 3066-3077.

Mathew, R., Kongara, S., Beaudoin, B., Karp, C. M., Bray, K., Degenhardt, K., ... & White, E. (2007). Autophagy suppresses tumor progression by limiting chromosomal instability. *Genes & development*, *21*(11), 1367-1381.

Medina, R. A., Goeger, D. E., Hills, P., Mooberry, S. L., Huang, N., Romero, L. I., ... & McPhail, K. L. (2008). Coibamide A, a potent antiproliferative cyclic depsipeptide from the Panamanian marine cyanobacterium Leptolyngbya sp. *Journal of the American Chemical Society*, *130*(20), 6324-6325.

Mizushima, N. (2004). Methods for monitoring autophagy. *The international journal of biochemistry & cell biology*, *36*(12), 2491-2502.

Mizushima, N., Yamamoto, A., Hatano, M., Kobayashi, Y., Kabeya, Y., Suzuki, K., ... & Yoshimori, T. (2001). Dissection of autophagosome formation using Apg5-deficient mouse embryonic stem cells. *The Journal of cell biology*, *152*(4), 657-668.

Nair, U., Yen, W. L., Mari, M., Cao, Y., Xie, Z., Baba, M., ... & Klionsky, D. J. (2012). A role for Atg8–PE deconjugation in autophagosome biogenesis. *Autophagy*, *8*(5), 780-793.

Nimmerjahn, F., Milosevic, S., Behrends, U., Jaffee, E. M., Pardoll, D. M., Bornkamm, G. W., & Mautner, J. (2003). Major histocompatibility complex class II-restricted presentation of a cytosolic antigen by autophagy. *European journal of immunology*, *33*(5), 1250-1259.

Sarkar, S. (2013). Regulation of autophagy by mTOR-dependent and mTOR-independent pathways: autophagy dysfunction in neurodegenerative diseases and therapeutic application of autophagy enhancers. *Biochemical Society Transactions*, *41*(5), 1103-1130.

Sehgal, S. N. (2003, May). Sirolimus: its discovery, biological properties, and mechanism of action. In *Transplantation proceedings* (Vol. 35, No. 3, pp. S7-S14). Elsevier.

Shen, H. M., & Codogno, P. (2011). Autophagic cell death: Loch Ness monster or endangered species?. *Autophagy*, *7*(5), 457-465.

Thornburg, C. C., Cowley, E. S., Sikorska, J., Shaala, L. A., Ishmael, J. E., Youssef, D. T., & McPhail, K. L. (2013). Apratoxin H and apratoxin A sulfoxide from the Red Sea cyanobacterium Moorea producens. *Journal of natural products*, *76*(9), 1781-1788.

Tsujimoto, Y., & Shimizu, S. (2005). Another way to die: autophagic programmed cell death. *Cell Death & Differentiation*, *12*, 1528-1534.

Xie, Z., Nair, U., & Klionsky, D. J. (2008). Atg8 controls phagophore expansion during autophagosome formation. *Molecular biology of the cell*, *19*(8), 3290-3298.

Yousefi, S., Perozzo, R., Schmid, I., Ziemiecki, A., Schaffner, T., Scapozza, L., ... & Simon, H. U. (2006). Calpain-mediated cleavage of Atg5 switches autophagy to apoptosis. *Nature cell biology*, *8*(10), 1124-1132.

APPENDIX

ddH_2O	3.3 mL

Tris-HCl (1.5M, pH 8.6)	2.5 mL
10% w/v SDS	50 µL
30% Acrylamide	4.2 mL
TEMED	5 uL
10% Ammonium Persulfate	50 uL

Per 10mL Resolving Gel

ddH_2O	3.0 mL
Tris-HCl (2M, pH 6.8)	1.25 mL
10% w/v SDS	25 µL
30% Acrylamide	0.75 mL
TEMED	5 µL
10% Ammonium Persulfate	25 µL

Per 5mL Stacking Gel

SDS	2 g
Tris (base)	0.76 g
2-mercaptoethanol	700µL

100mL Stripping buffer

NaCl	8 g
KCl	0.2 g
$Na_2HPO_4 \bullet 7H_20$	2.73 g
KH_2PO_4	0.24 g

Per liter of 1x Phosphate buffered saline (PBS)

NaCl	8 g
KCl	0.2 g
Tris (Base)	3 g
HCl	Bring to pH 7.4
Tween-20	0.5 mL

Per liter of 1x TBST

Glycine	14.4 g
Tris (Base)	3.03 g
SDS	1 g

Per liter of running buffer

Tris (Base)	3.03 g
Glycine	14.4 g
Methanol	100 mL

Per liter of electrotransfer buffer

Tris-HCl (1M, pH 7.5)	0.5 mL
EGTA (0.5M)	20 µL
EDTA (0.5M)	20 µL
Triton X-100 (10%)	1 mL
Sucrose	0.93 g
Na_3VO_4 (100nM)	100 µL
$Na_4(PO_4)_2$	0.022 g
Benzamidine (1mM in 10mL)	20 µL
PMSF (100mM in 10 mL)	20 µL

Per 10 mL cell lysis buffer

DMEM	13.49 G
Sodium Bicarbonate	49.3 mL
Penicillin / Streptomycin	5 mL
FBS	100 mL

Per 1L DMEM

Tris (pH 6.8)	0.8M
SDS (w/v)	8%
EDTA	5mM
Glycerol	40%
DTT	0.2 M

4x Laemmli buffer